

## Lubrication State on the Sliding Part of a Multiple Vane Type Compressor

Eita KUREHA \*1 and Masayoshi MURAKI\*2

\*1 Research Center, Research and Development Center, Yanmar Co., Ltd.  
1600-4, Umegahara, Maibara-shi, Shiga 521-8511, JAPAN  
EITA\_KUREHA@yanmar.co.jp

\*2 Department of Mechanical Engineering, Shonan Institute of Technology  
1-25, Tsujido-nishikaigan 1-chome, Fujisawa-shi, Kanagawa 251-8511, JAPAN  
muraki@mech.shonan-it.ac.jp

### Abstract

Excessive wear of sliding part of a multiple vane type compressor after its long-period use in HCFC-22 was reported in some operating conditions. Then, influence of refrigerant gas on wear of sliding material was studied with a test rig. As a result, the wear amount in HCFC-22 was much larger than that in HFC-134a and air because of corrosive wear under the severe conditions. Then, oil film formation on the top of vane was evaluated as the separation degree using the compressor equipped with an electrical insulating circuit. The separation degree decreased with a decrease in oil supply quantity and with an increase in suction pressure. In order to study the influence of suction pressure, the parameters affecting oil film formation were determined by taking into consideration the force balance around vane. The calculated oil film parameter  $\Lambda$  could be obtained. Change in  $\Lambda$  with suction pressure qualitatively showed a good agreement with that of separation degree.

**Keywords:** multiple vane type compressor, refrigerant, lubrication, oil film parameter, suction pressure

### 1 Introduction

Since a multiple vane type compressor, in Fig.1, is composed of a cylinder and a rotor installed on the same shaft, the load unbalance during rotation is low compared to the other types, which enables high rotational speeds. Consequently, a high capacity at a small size, and low vibration leads to wide applications such as automobile air conditioners and gas heat pumps

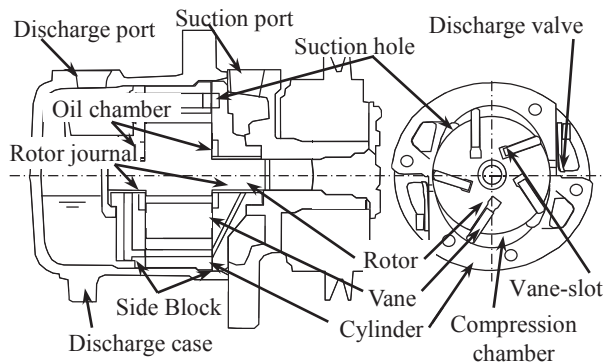


Fig.1 Structure of multiple vane type compressor

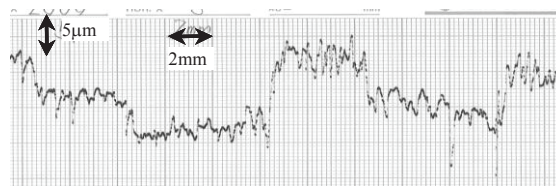


Fig.2 Surface profile on cylinder compression part of on-market product operated over 5000hr

of an engine driving system. However, excessive wear of cylinder inside was reported after long-period use under specific condition in the actual application. Figure 2 shows the surface profile on the compression stroke part of cylinder inside made of cast iron, which shows formation of large steps due to wear.

There are some studies which report about the lubrication phenomena of compressors [1] [2]. On the other hand, there are few references which describe with detail about a set of lubrication evaluations of compressors for air conditioner designers.

In the present paper, first wear properties of vane and cylinder material under refrigerants are studied, and then the effect of oil supply and suction pressure on oil film formation was evaluated. The parameters affecting oil film formation are determined based on force balance around vane. Finally, the relationship between oil film formation and calculated film parameter is discussed in terms of effect of suction pressure.

### 2 Wear of cylinder material

#### 2.1 Experimental

Influence of refrigerant gas on the wear of a combination of vane and cylinder were studied with an aluminum alloy pin-on-cast iron disk type tribometer equipped, as shown in Fig.3. The test part is in a pressure container.

Experiments were carried out under the sliding speed of 0.5m/s, the load of 1500N, the oil temperature of 80°C and the refrigerant gas pressure of 500kPa absolute for the test period of 60minutes. The lubricant was polyalkylene glycol whose kinematic viscosity was 143mm<sup>2</sup>/s at 40°C and 25mm<sup>2</sup>/s at 100°C.

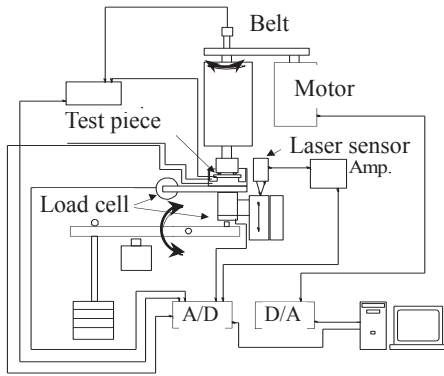


Fig.3 Pin on disk type tester

## 2.2 Test results

Figure 4 compares the wear depth of the cast iron disk between environment gases. The wear depth is the largest for HCFC-22, followed by HFC-134a and air.

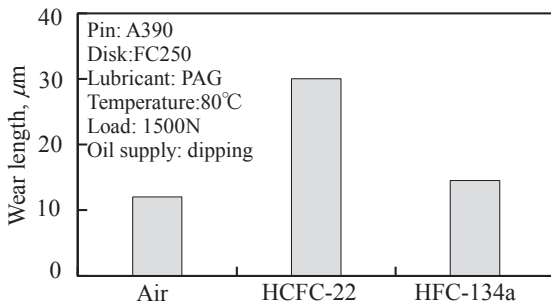


Fig.4 Effect of atmospheric gas

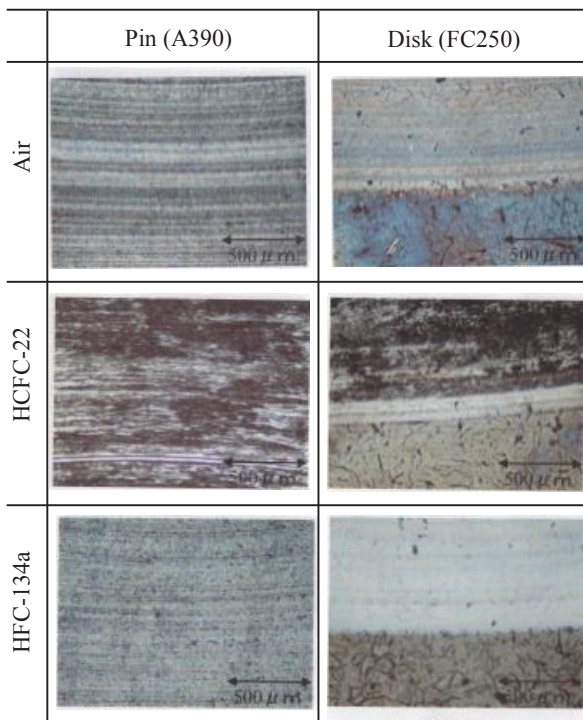


Fig.5 Sliding surfaces after tests

The sliding surfaces of the test specimens were observed with an optical microscope, as shown in Fig.5. Slight wear scratches along the sliding direction are observed on the surfaces in both air and HFC-134a and the color of the surfaces is white or light blue. On the other hand, the sliding surface in HCFC-22 is rough and black.

It has been generally accepted that HCFC-22 is superior to HFC-134a in terms of antiwear performance because chlorine in refrigerant is decomposed to react the metal surface and to form iron chloride reacts as an extreme pressure agent. The opposite results in the present study suggests that decomposed chlorine promoted the corrosive wear. That is, it is inferred that excessive wear of cast iron under HCFC-22 in the actual application occurred under severe contact conditions.

## 3 Oil film formation on the top of vane

### 3.1 Separation degree

Electrical contact resistance (ECR) method was employed to estimate the extent of oil film formation on the top of vane, as shown in Fig.6. A voltage of 200mV was applied between the cylinder and the vane. Figure 7 exhibits the result obtained by JIS standard measurement conditions for cooling. In the figure, a separation degree ( $SD$ ) is defined as percentage of the measured voltage to applied voltage.

The value of  $SD$  in suction period shows almost full level, suggesting the sufficient lubrication state. Since this tendency was common to all the operating conditions, the extent of oil film formation was evaluated as an averaged separation degree ( $ASD$ ) during compression and discharge period corresponding to the rotor angle from  $90^\circ$  to  $150^\circ$ .

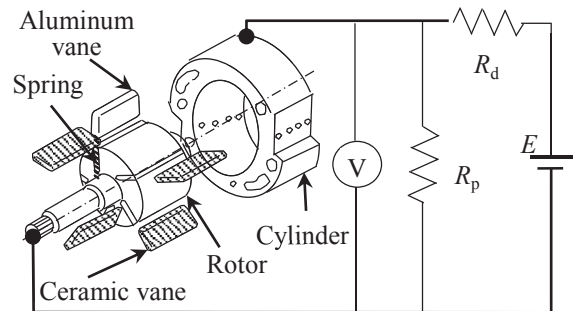


Fig.6 Electrical contact resistance method

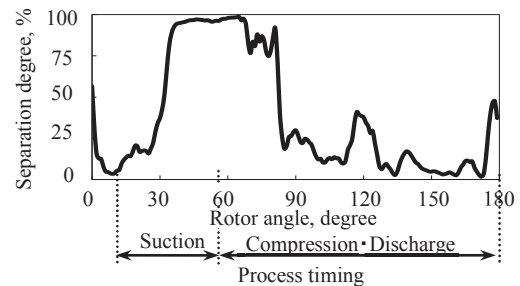


Fig.7 Variation in  $SD$  with rotor angle

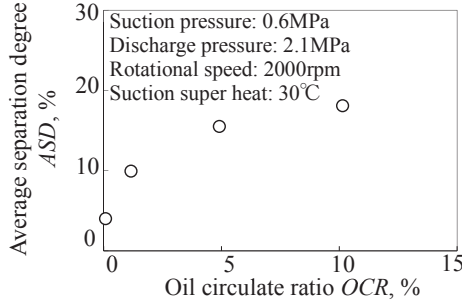


Fig.8 Effect of OCR on ASD

### 3.2 Effect of oil circulation ratio

The oil supply quantity to the top of vane was studied by adjusting oil circulation ratio  $OCR$ , in which  $OCR$  was defined as the ratio of circulating oil flow to circulating refrigerant flow.

Figure 8 shows the effect of  $OCR$  on  $ASD$ . As  $OCR$  increases,  $ASD$  first increases, and then it tends to level off. This suggests that a sufficient oil film formation can be obtained on the condition of  $OCR$  more than 5%. This can be easily understood that an increase in  $ASD$  was brought about by increase in oil supply.

### 3.3 Effect of suction pressure

Next, the effect of suction pressure on  $ASD$  was studied under the real field conditions. As will be shown later,  $ASD$  deteriorates with increasing suction pressure. This is because change in suction pressure causes change in some parameters affecting oil film formation on the top of vane. Thus, such parameters have to be determined by taking into consideration the force balance around vane.

## 4 Dynamic model around vane

The forces acting on vane are shown in Fig.9. The original point of rotor angle was defined as the minor axis of cylinder.

In compression period, vane is subject to huge momentum by the differential force ( $P_{cf} - P_{cr}$ ). The momentum is supported by  $F_1$  and  $F_2$ . After vane cross the major axis of cylinder (rotor angle of 90 degree), the oil film on the working point of  $F_1$  is formed by the wedge action. In the contact part of vane on the vane slot, it is considered that  $F_1$  is supported by oil film force ( $F_{of1}$ ) and direct contact force ( $F_{c1}$ ).  $F_{of1}$  was calculated by infinite width theory. Meanwhile,  $F_{c1}$  was calculated based on the mixed lubrication theory using GT model [3]. Thus,  $\mu_1 F_1$  is expressed as follow,

$$\mu_1 F_1 = \mu_b F_{c1} + F_{\tau-oil} \quad (1)$$

$$F_1 = F_{c1}(A) + F_{of1}(A) \quad (2)$$

where  $\mu_b$  is the boundary friction coefficient, and  $F_{\tau-oil}$  is the shear resistance of an oil film.

On the other hand,  $F_2$  is assumed to be supported only by direct contact force. Finally,  $F_n$  can be obtained based on the force balance along  $x$ -direction forces ( $P_{cf}$ ,  $P_{cr}$ ,  $P_o$ ,  $\mu_1 F_1$ ,  $\mu_2 F_2$ ). In addition, it is considered that  $F_n$  is also supported by oil film reaction force calculated by Martin's equation and direct contact

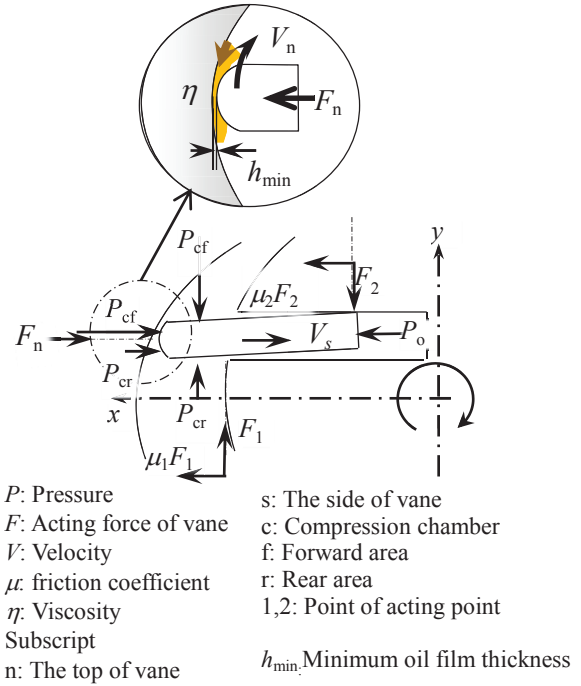


Fig.9 Dynamical model around vane

force. On the basis of the force balance around the vane, the parameters affecting oil film formation on the top of vane are pressure in compression chamber  $P_{cf}$  and  $P_{cr}$ , pressure in oil chamber  $P_o$ , the viscosity of refrigerant/oil mixture and the boundary friction coefficient  $\mu$ . The viscosity for calculation of oil film thickness was obtained by the theoretical pressure and temperature in the forward compression chamber.

## 5 Parameters affecting oil film formation

### 5.1 Pressure in compression chamber $P_c$

$P_c$  influences  $F_1$ ,  $F_2$ , and  $\eta$ , and acts in the opposite direction of  $F_n$ . Therefore,  $P_c$  has to be estimated accurately. The compression chamber rotates with rotating rotor, so  $P_c$  was measured by installing five pressure sensors in this compressor.  $P_c$  over one cycle is obtained by combining five datum of pressure sensors, as shown Fig.10. It is identified that the over-compression is high, and that the pressure until the maximum pressure can be predicted by theoretical adiabatic compression.

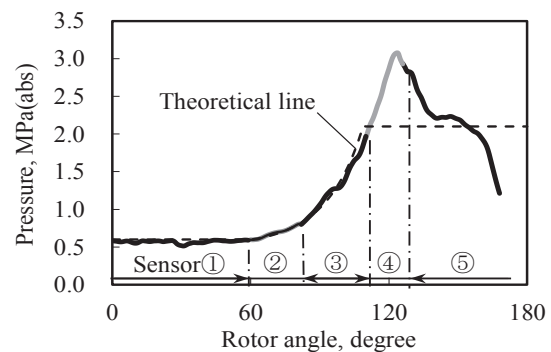


Fig.10 Variation in pressure with rotor angle

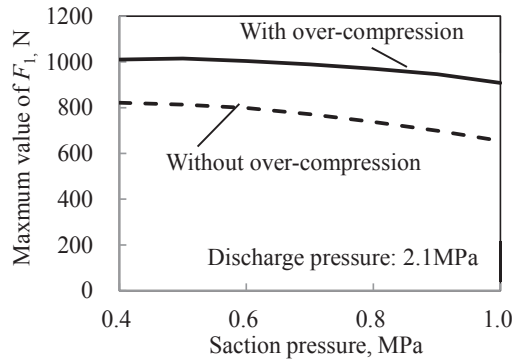


Fig.11 Effect of over-compression

Figure 11 shows that the over-compression increases  $F_1$  significantly, it can be predicted that  $\mu_1 F_1$  and  $F_n$  increases largely.

### 5.2 Pressure in oil chamber $P_o$

The back of vane is pushed by oil pressure in oil chamber. The oil supplied in oil chamber flows along the pathway shown in Fig.12. The quantity of flow and the local pressures are determined by the flow resistances in rotor-journals and rotor-sides. The quantity of flow from discharge case to oil chamber ( $Q_1$ ) and that from oil chamber to compression chamber ( $Q_2$ ) are expressed as below equations [4].

$$Q_1 = n_1 \frac{\pi d C_j^3}{12 \eta L} (P_d - P_o) \quad (3)$$

$$Q_2 = n_2 \frac{\pi d C_r^3}{6 \eta \ln(R_r/R_o)} (P_o - P_{meanc}) \quad (4)$$

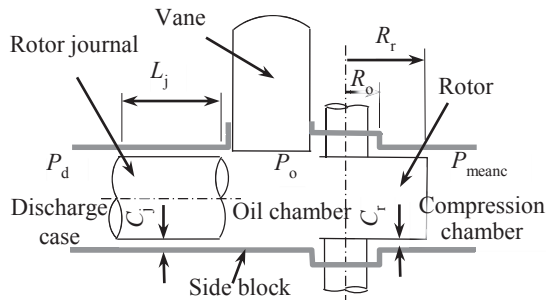


Fig.12 Pathway of oil

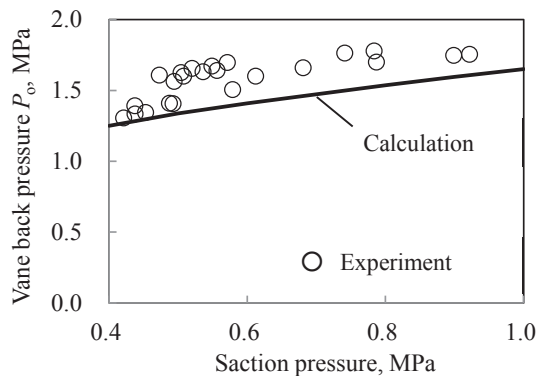


Fig.13 Calculation result of  $P_o$

where  $n_1$  and  $n_2$  are number of the pathways, and  $P_{meanc}$  is average pressure along outer circumferential of rotor.

$P_o$  can be calculated from eq. (3) and eq. (4), as  $Q_1$  is equal to  $Q_2$  under the law of conservation of mass. Comparison between calculated  $P_o$  and measured  $P_o$  is shown in Fig.13. The calculation results exhibit the same tendency of the experimental result, so the calculation method proved reasonable.

### 5.3 Viscosity of refrigerant/oil mixture

Refrigerant is soluble in oil so that the viscosity of refrigerant/oil mixture varies depending on the solubility properties of refrigerant.

The temperature-pressure-viscosity relations of refrigerant/oil mixture were obtained with a falling piston type viscometer as shown in Fig.14. Figure 15 shows the viscosity-temperature relation as a parameter of refrigerant gas pressure. It can be seen that the viscosity decreases around the saturated temperature of refrigerant rapidly due to high solution of refrigerant.

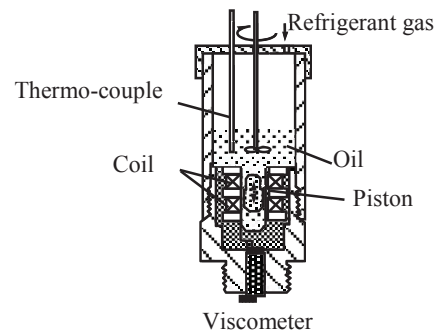


Fig.14 Viscometer for refrigerant/oil mixture

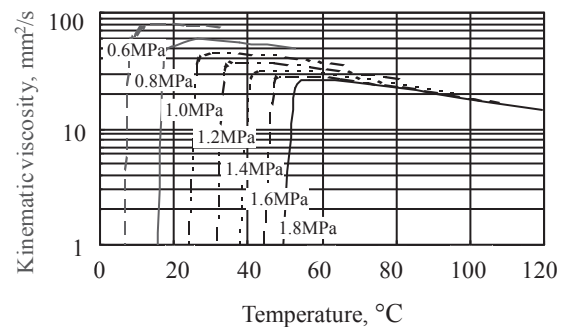


Fig.15 Viscosity-temperature-pressure relation of refrigerating lubricant

### 5.4 Friction coefficient $\mu$

The force  $F_n$  is affected by the friction coefficient for aluminum alloy versus steel at the operating point of  $F_1$ . Boundary friction coefficient under severe lubrication condition was experimentally determined with the pin on disk type tester as mentioned in the former chapter. As shown in Fig.16, the boundary friction coefficient shows around 0.12 under flooded condition, and then it reaches 0.25 because of starved condition.

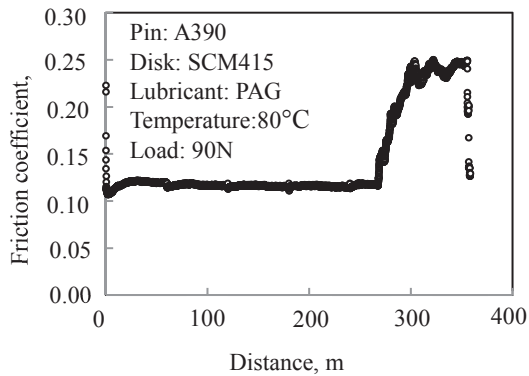


Fig.16 Friction coefficient on vane-slot

## 6 Comparison between ASD and $\Lambda$

Figure 17 shows that *ASD* expressing the extent of oil film formation on the top of vane deteriorates with increasing suction pressure. In the figure, oil film parameter  $\Lambda$  as calculated results is also depicted, where  $\Lambda$  is defined by the ratio of the oil film thickness to the composite roughness of the sliding surfaces. And the oil film thickness was calculated by using the above mentioned parameter. As is seen in the figure, the calculated results exhibit the same tendency to the experimental results. That is, the proposed methods of the parameters are appropriate for preventing excessive wear of the sliding part and design of refrigerating machines.

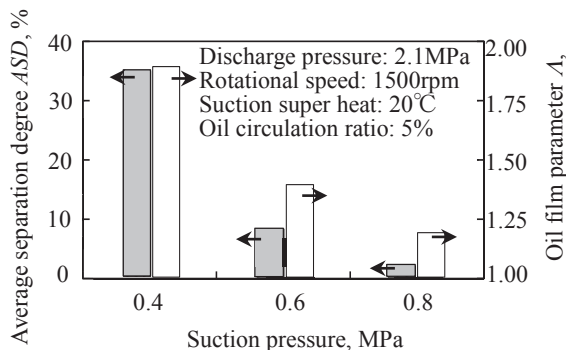


Fig.17 Comparison between experimental and calculated results

## 7 Conclusions

The lubricant state on the top of vane of a multiple vane type compressor was experimentally determined as separation degree. Meanwhile, the parameters affecting oil film formation were clarified and their measuring techniques were proposed. The main results are as follows.

- The wear amount in HCFC-22 was much larger than that in HFC-134a because of corrosive wear based on formation of iron chloride from HCFC-22 under the severe conditions.
- The extent of separation degree decreases with decreasing oil circulation ratio and increasing suction pressure.
- By analyzing the force balance around vane based on the mixed lubrication theory, the parameters affecting oil film formation were clarified. They were the pressure in compression chamber, pressure in oil chamber, the boundary friction coefficient and the viscosity of refrigerant/oil mixture.
- The oil film parameter calculated using necessary parameters agreed well with the separation degree in terms of effect of suction pressure.

## References

- S. Tanaka, K. Kyogoku, and T. Nakahara, "Lubrication Characteristics of Refrigerator / Air conditioning Rotary Compressor": JAST, Vol.41, No.3, (1996), pp.247-254.
- T. Yoshimura, K. Ono, K. Inagaki, H. Kotsuka, and A. Korenaga, "Analysis of Lubricating Characteristics of Rotary Compressor for Domestic Refrigerators": Transaction of the ASME, Journal of Tribology, Vol.122, No.7, (1999), pp.510-516.
- Y. Ito, H. Hattori, K. Miura, and T. Hirayama, "Mixed Lubrication Analysis of Vane Sliding Surface in Rotary Compressor Mechanisms": Tribology Online, Vol.2, No.3, (2007), pp.73-77.
- M. Fukuta, T. Yanagisawa, M. Ijiri, and S. Yoda, "Vane Back-Pressure of Vane Type Compressors and Its Mathematical Model": JSRAE, Vol.20, No.3, (2003), pp.375-385.

Received on October 30, 2013

Accepted on January 22, 2014